

High-field electrical transport and breakdown in bundles of single-wall carbon nanotubes

M. Radosavljević, J. Lefebvre, and A. T. Johnson

Department of Physics and Astronomy and Laboratory for Research on the Structure of Matter, University of Pennsylvania, Philadelphia, Pennsylvania 19104

(Received 16 July 2001; published 4 December 2001)

We investigate high-field transport in bundles of single-wall carbon nanotubes (SWNTs) with multiple contacts. The bundles carry currents in excess of 250 μA (a current density of 10^9 A/cm^2) before saturation and electrical breakdown, indicating that conduction is predominantly by nanotubes on the surface of the bundle which are directly contacted by electrodes. Using a four-probe configuration, we measure the contact resistance and show that it is nearly constant as the bias voltage varies. This strongly supports the notion that electron-phonon scattering, and not a contact effect, causes current saturation at high-field. Electrical breakdown proceeds by sequential destruction of individual metallic nanotubes on the bundle surface, with steplike current drops of about 12 μA . At very high bias, the current-carrying capacity of the bundle increases due to field-enhanced coupling between nanotubes in the bundle.

DOI: 10.1103/PhysRevB.64.241307

PACS number(s): 73.50.-h, 73.63.Fg, 73.23.-b, 73.50.Fq

Single-wall carbon nanotubes (SWNTs) are a leading candidate for molecular electronic circuit elements.¹ Individual semiconducting SWNTs act as field-effect transistors² and diode-like rectifiers,³ while metallic SWNTs behave as single-electron transistors.⁴ Recent studies of metallic SWNTs in the high-field regime report a current saturation with maximum current density exceeding 10^9 A/cm^2 .⁵ Such high current carrying capacity is similar to that seen in multiwall carbon nanotubes^{6,7} (MWNTs) and as much as a thousand times greater than in noble metals. Thus, metallic SWNTs and MWNTs are promising nanometer-scale circuit interconnects.

Here we present results on high-field transport in bundles of SWNTs with a focus on the mechanism of current saturation and field-induced electrical breakdown. A multiprobe geometry was used to directly measure the contact resistance and show that electron-phonon scattering is the dominant mechanism leading to current saturation,⁵ not a contact effect as others have suggested. Bundles of SWNTs do not fail via electromigration⁸ which limits the current-carrying capacity of conventional wires. Instead, the breakdown occurs by individual, sharp current drops of about 12 μA , which we identify with the destruction of individual current-carrying nanotubes. Such a “current staircase” was observed in multiwall carbon nanotubes and is attributed to the destruction of individual shells.⁷ At low field, we find that the coupling between nanotubes in the bundle is weak, and the current is carried predominantly by nanotubes on the surface of the bundle which are in direct contact with the electrodes.^{9,10} At high bias just before complete breakdown, we observe an additional current increase which is caused by the coupling to the nanotubes in the interior of the bundle.

Devices are produced by depositing ethanol dispersion of laser-ablation grown SWNT material¹¹ onto a SiO_2 substrate. Bundles of uniform size are located and contacted by four electrodes using standard nanofabrication techniques.¹² The large 2 μm wide outer electrodes (source and drain) are 3–5 μm apart and cover a significant length of the bundle including both ends. Although this design was intended to facilitate current flow in the bulk of the sample, we find that

the current is confined to the nanotubes which are in direct contact with source and drain electrodes.¹⁰ The voltage probes are 300 nm wide and within 500 nm of the outer electrodes, insuring that the measurements are representative of the whole sample. The bundles exhibit a wide variety of low-field¹⁰ behavior in part due to the fact that each bundle contains nanotubes with randomly distributed chiralities.^{13,14} To study high-field behavior and breakdown, we focus on “metallic” bundles that show weak response to electrostatic gating at room temperature and whose low bias resistance decreases linearly with decreasing temperature.¹⁰ The contact resistance to these devices is below 3 k Ω at low-field, so 50%–70% of the applied voltage drops along the bundle. The experiments are performed by applying a voltage (V_A) between the source and the drain while measuring the current (I) passing through the sample and the voltage drop (V_M) between the two middle electrodes [inset to Fig. 1(a)].

Figure 1(a) is the two-probe current-applied voltage ($I - V_A$) characteristic obtained at ambient conditions of a 22 nm tall SWNT bundle with a 2.6 μm separation between the middle electrode pair.¹⁵ A current of 180 μA is measured at the largest applied bias of 2.25 V. The differential conductance (dI/dV) is approximately constant for applied biases up to 0.5 V, at which point it begins to decrease slowly. The shape of the $I - V_A$ above 0.5 V suggests an onset of current saturation at high bias. Figure 1(b) displays the simultaneously acquired (four probe) current-measured voltage ($I - V_M$) characteristic. Here, the conductance begins to decrease at a much lower voltage of 0.15 V, and the current seems to saturate at a much lower value than in Fig. 1(a). Although the low-field resistance decreases linearly with decreasing temperature,¹⁰ the behavior at large bias is unchanged as these devices are cooled to 4 K.

In order to determine the origin of current saturation, we plot the current-contact voltage ($I - V_C$) characteristic in Fig. 2. V_C is defined as the total voltage drop across the contacts between the bundle and the two outmost electrodes. We find the contact voltage using the following formula:

$$V_C = V_A - \alpha V_M, \quad (1)$$

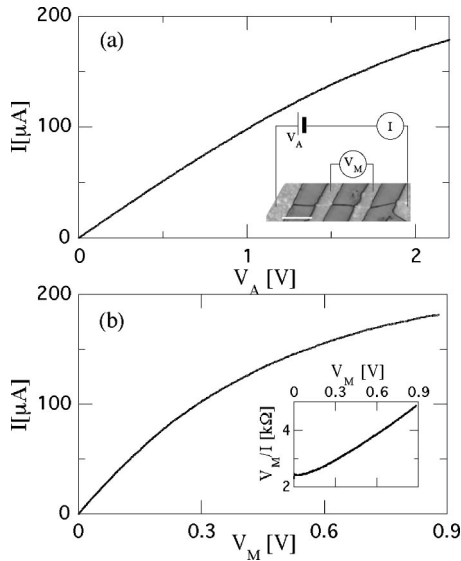


FIG. 1. High-field behavior of a 22 nm tall SWNT bundle measured in a four-probe configuration. (a) Two-probe $I-V_A$. Inset: AFM image of SWNT bundle contacted by four electrodes and schematic of the measurement. The white bar in the AFM image is 2 μm . (b) Simultaneously acquired four-probe $I-V_M$ measured using the middle electrode pair (2.6 μm separation). Inset: V_M/I vs V_M . The linear region is a signature of current saturation by optical phonon emission. A fit to Eq. (2) yields a saturation current of 250 μA .

where $\alpha \geq 1$ accounts for the voltage drop along the portion of the bundle that lies outside the voltage probes. Assuming that the voltage drops uniformly along the bundle in the high-field regime,¹⁶ then α is determined by the contact geometry. A reasonable value of $\alpha = 1.5$ is used to plot Fig. 2. The $I-V_C$ curve is almost perfectly linear, indicating that the contact resistance (V_C/I) is constant over the whole bias range studied. Additionally, the linearity of the $I-V_C$ is not sensitive to different values chosen for the parameter α . Therefore, we conclude that the current saturation observed in Fig. 1 is intrinsic to the bundle and not caused by the nonlinear behavior of the contacts.

Theoretical investigations of high-field behavior in nano-

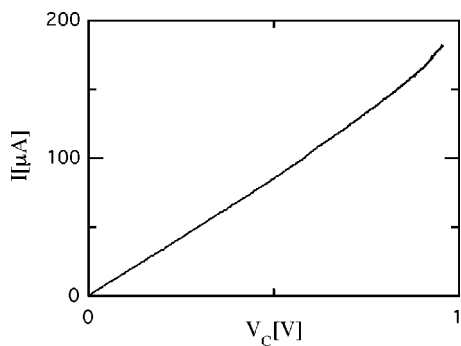


FIG. 2. Inferred current-voltage characteristic of the source and drain contacts. V_C is computed using Eq. (1). The $I-V_C$ is linear, verifying that the high-field current saturation is not caused by the contacts, but instead an effect intrinsic to the SWNT bundle, most likely excitation of high energy optical phonons.

tubes focus on two intrinsic effects: electron scattering by optical phonon emission⁵ and transport through higher, non-crossing nanotube subbands.¹⁷ Our measurements deviate from linear response at energies that are much lower than the typical first subband separation of 2 eV. We, therefore, direct our attention to the impact of electron backscattering due to emission of optical phonons with energy $\hbar\Omega \sim 160$ meV, appropriate for a stretch of the carbon-carbon bond. The model developed by Kane⁵ considers a steady state situation where the right-moving electrons have a Fermi energy $\hbar\Omega$ higher than the left-movers. Right-moving electrons are accelerated by the electric field in the nanotube and are subsequently backscattered into the left-moving branch with the excess energy released as an optical phonon. Using a Landauer type argument and Boltzmann transport theory, Kane predicts a precise form for the $I-V$ characteristics:

$$R \equiv V/I = R_0 + V/I_0. \quad (2)$$

The low-field elastic (defect) scattering within the nanotube is described by the constant R_0 , while $I_0 = (4e^2/h)(\hbar\Omega/e)$ is the saturation current. The theoretical prediction $I_0 = 25 \mu\text{A}$ per nanotube is consistent with the experiment.⁵

Using Eq. (2), we obtain $I_0 \sim 250 \mu\text{A}$ from $I-V_M$ data [Fig. 1(b)], indicating that the current is carried by 10 metallic nanotubes¹⁸ while the total number of tubes in the bundle (from its diameter of 22 nm) is a few hundred. Therefore, current is limited to nanotubes on the bundle surface that are in direct contact with source and drain.^{9,10}

To come to these conclusions, one must accurately infer I_0 from the data. Most critically, the value of V used in Eq. (2) is the voltage drop *along* the bundle, without a contribution from the contact. For this reason, the fit to the *four-probe* $I-V_M$ is used to obtain saturation current, *not* the fit to the two-probe $I-V_A$. We expect theoretically, and in fact find experimentally, that if the two-probe $I-V_M$ data is used, the excess voltage at the contacts leads to an incorrectly large value for I_0 .¹⁹ As we discuss below, electrical breakdown occurs at current levels smaller than our inferred saturation current, so we do not observe the saturation current directly. However, our measurements of the saturation current from the $I-V_M$ before and following a breakdown event (see Fig. 4) is consistent with an ideal saturation current of 25 μA per tube.

Figure 3 shows a bundle $I-V_A$ during electrical breakdown event. As the voltage is increased, an irreversible current drop is observed at $V_A \sim 1.3$ V. The current drop of 12 μA occurs on a time scale faster than the data acquisition rate (40 ms per point). Subsequent bias sweeps show decreased current carrying capacity indicating permanent damage to the SWNT bundle. A similar current staircase due to successive shell destruction has been recently observed in multiwall carbon nanotubes.⁷

In order to elucidate the cause of the electrical breakdown, the inset to Fig. 3 compares four-probe $I-V_M$ before and after the current drop (labeled 1 and 2, respectively). At high field, the saturation currents [determined using Eq. (2)]

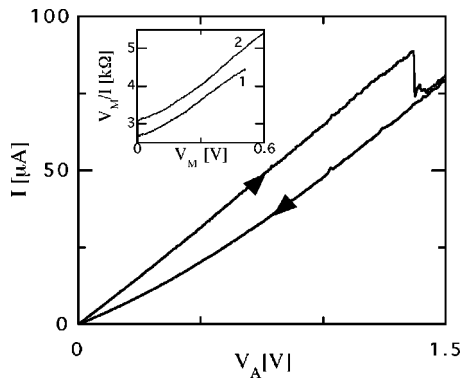


FIG. 3. Observation of electrical breakdown in SWNT bundles. The two probe $I-V_A$ shows a sudden irreversible drop in current of approximately $12 \mu\text{A}$. Inset: four-probe data before and after electrical breakdown, labeled 1 and 2, respectively. Fits to Eq. (2) yield saturation currents of $250 \mu\text{A}$ before breakdown, and $223 \mu\text{A}$ after. The $27 \mu\text{A}$ decrease in current carrying capacity indicates that the current drop is due to destruction of an individual metallic SWNT.

are $250 \mu\text{A}$ before breakdown and $223 \mu\text{A}$ after. We interpret the step as the destruction of precisely one metallic nanotube on the surface of the bundle, and the $27 \mu\text{A}$ decrease in the current is in good agreement with the theoretical prediction of $25 \mu\text{A}$. The difference between the current carrying capacity of an individual SWNT ($25 \mu\text{A}$) and the observed current drop ($12 \mu\text{A}$) is likely because the active SWNTs in the bundle carry different currents. Only a SWNT in saturation suffers breakdown, and a fraction of its current is then redistributed among the other SWNTs.

Figure 4 displays four $I-V_M$ characteristics separated by three breakdown events. The current reductions associated with each breakdown are $25 \mu\text{A}$, $12 \mu\text{A}$, and $36 \mu\text{A}$, respectively. Complete breakdown occurred after the fourth $I-V_M$. The breakdown always happens after the onset of current saturation, consistent with the idea that the electrical breakdown and current saturation are due to the same dissipative process. Interestingly, the $I-V_M$ curves are not smooth, but contain abrupt slope changes. The most prominent kink occurs near 3.75 V in curve 3, where the current appears to saturate near $200 \mu\text{A}$ only to abruptly increase and saturate again at $250 \mu\text{A}$ at higher voltage. This increase in current-carrying capacity indicates that the number of conducting channels within the bundle has increased. We believe that these additional channels are metallic SWNTs in the core of the bundle, which are not directly contacted by source and drain electrodes. Our observation confirms that at high-field, many nanotubes carry current in a SWNT bundle, while at low-field the current is localized on just a few nanotubes.^{9,10} This difference may well reflect the energy dependence of intertube coupling, which has been considered theoretically only in the low energy limit.¹⁴ However, we expect that at high bias, intertube coupling is enhanced

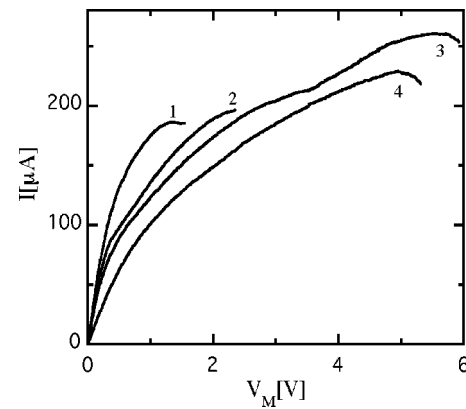


FIG. 4. $I-V_M$ curves measured following successive breakdown events (curves are numbered in order taken). Complete breakdown occurs after the fourth sweep. $I-V_M$ curves in breakdown sequence contain abrupt slope changes. Such kinks result in an increased saturation current suggestive of additional conduction channels, most likely nanotubes within the core of the bundle.

due to the relaxation of momentum conservation among nanotubes and an increase in electron-electron scattering.

After complete breakdown, no current passes between the middle electrode pair for biases up to 5 V . In contrast, two-probe $I-V$ characteristics of bundle segments outside the middle electrodes are unchanged, indicating that the damage is confined to the central region of the sample. In addition, AFM images (not shown) of failed SWNT bundles reveal large quantities of lost carbon between the middle electrode pair. The remaining bundle is severely thinned between the electrodes, consistent with breakdown due to self-heating. Estimating the SWNT thermal conductivity in SWNT bundles as 250 W/m-K^{20} and the observed power threshold ($350\text{--}1000 \mu\text{W}$), we compute a bundle temperature of $600\text{--}800^\circ\text{C}$, comparable to the temperature needed for thermal oxidation of SWNTs. Initial measurements of the local temperature distribution along a nanotube²¹ confirm that the temperature is elevated by $100\text{--}200 \text{ K}$ at moderate applied biases.

In summary, we have measured the high-field conduction limits of SWNT bundles. A multiprobe geometry was used to measure the contact resistance directly and show that current saturation is due to an intrinsic effect that is likely optical phonon emission. The high-field breakdown of SWNT bundles occurs by the destruction of individual, current-carrying nanotubes. At the highest biases, an observed current increase suggests conduction through metallic SWNTs within the core of the bundle.

We thank C. Kane for helpful discussions, and M. Freitag and P. Collins for sharing experimental results prior to publication. SWNT material was provided by the Smalley group (Rice University). Financial support for this work came from NSF grants DMR98-02560 and DMR00-79909. J.L. recognizes the support of Fonds FCAR (Québec).

- ¹C. Dekker, Phys. Today **52**, 22 (1999); P.L. McEuen, Phys. World **13**, 31 (2000).
- ²S.J. Tans, A.R.M. Verschueuren, and C. Dekker, Nature (London) **393**, 49 (1998); R. Martel *et al.*, Appl. Phys. Lett. **73**, 2447 (1998).
- ³R.D. Antonov and A.T. Johnson, Phys. Rev. Lett. **83**, 3274 (1999); Z. Yao *et al.*, Nature (London) **402**, 273 (1999); M. Fuhrer *et al.*, Science **288**, 494 (2000).
- ⁴S.J. Tans *et al.*, Nature (London) **386**, 474 (1997); M. Bockrath *et al.*, Science **275**, 1922 (1997).
- ⁵Z. Yao, C.L. Kane, and C. Dekker, Phys. Rev. Lett. **84**, 2941 (2000).
- ⁶H. Dai, E.W. Wong, and C.M. Lieber, Science **272**, 523 (1996); S. Frank *et al.*, *ibid.* **280**, 1744 (1998).
- ⁷P.G. Collins *et al.*, Phys. Rev. Lett. **86**, 3128 (2001); P.G. Collins, M.S. Arnold, and Ph. Avouris, Science **292**, 706 (2001).
- ⁸A. Christou, *Electromigration and Electronic Device Degradation* (Wiley-Interscience, New York, 1994).
- ⁹H. Stahl *et al.*, Phys. Rev. Lett. **85**, 5186 (2000).
- ¹⁰J. Lefebvre, M. Radosavljević, J. Hone, and A. T. Johnson (unpublished).
- ¹¹A. Thess *et al.*, Science **273**, 483 (1996).
- ¹²J. Lefebvre *et al.*, Appl. Phys. Lett. **75**, 3014 (1999).
- ¹³L. Henrard *et al.*, Synth. Met. **103**, 2533 (1999).
- ¹⁴A.A. Maarouf, C.L. Kane, and E.J. Mele, Phys. Rev. B **61**, 11 156 (2000).
- ¹⁵Measured $I-V$ characteristics are all symmetric about the origin. We plot only the positive values for clarity.
- ¹⁶Conducting tip-AFM measurements performed in our laboratory show that the voltage drops uniformly along an individual SWNT at high bias, thus confirming our assumption.
- ¹⁷M.P. Anantram, Phys. Rev. B **62**, R4837 (2000).
- ¹⁸Semiconducting SWNTs do not contribute strongly to the high-field transport because they are not conducting at zero gate voltage. However, high-field behavior in semiconducting SWNTs is poorly understood and is currently under investigation.
- ¹⁹This computation is performed assuming constant contact resistance as observed in our experiments. The amount by which saturation current is overestimated is proportional to the ratio of the contact voltage to the applied bias. In typical samples, the error can range from 50% to a factor of 2.
- ²⁰J. Hone *et al.*, Appl. Phys. Lett. **77**, 666 (2000).
- ²¹P. Kim, L. Shi, A. Majumdar, and P.L. McEuen, Phys. Rev. Lett. **87**, 215502 (2001).